Available online at www.sciencedirect.com
SCIENCE DIRECT®
Physica B 336 (2003) 267–274
PHYSICA B
www.elsevier.com/locate/physb

Magnetoresistance of $La_{0.7}Ca_{0.3}MnO_3$ thin film biepitaxial step junctions

S.F. Chen[a,*], W.J. Chang[a], S.J. Liu[a], J.Y. Juang[a], J.-Y. Lin[b], K.H. Wu[a], T.M. Uen[a], Y.S. Gou[a]

[a] *Department of Electrophysics, National Chiao Tung University, 1001 Ta Hsueh Road, Hsinchu 300, Taiwan*
[b] *Institute of Physics, National Chiao Tung University, Hsinchu 300, Taiwan*

Received 27 January 2003; accepted 8 April 2003

Abstract

The biepitaxial $La_{0.7}Ca_{0.3}MnO_3$ (LCMO) thin films grown on $SrTiO_3$ substrates using a buffer layer of anatase TiO_2 were fabricated. The magnetoresistance (MR) of biepitaxial step junction (BSJ) across the boundary layer of biepitaxial LCMO (0 0 1) and LCMO (1 1 0) film was investigated. The temperature and field dependence of MR for BSJ are qualitatively similar to those obtained in other type of artificial grain boundaries with a comparable MR ratio at low temperatures. However, the observed linear current–voltage characteristic across BSJ is in sharp contrary to the commonly reported non-ohmic characteristics. The results are consistent with features predicted by the model of spin-dependent transport across a depressed magnetic ordering and metallic-like junction layer.

PACS: 72.25.−b; 75.30.Vn

Keywords: Magnetoresistance; Biepitaxial step junction; LCMO; Grain boundary

1. Introduction

The observation of colossal magnetoresistance (CMR) in perovskite manganites has led considerable interest due to its potential applications in magnetic controllable electronic devices. Unfortunately, a large magnetic field (several Tesla) is required to achieve over 10 percent of resistance change in manganite materials, making it difficult to use this intrinsic magnetoresistance (MR) property directly for device designing. Thus, devices, which can achieve a large MR ratio with a low magnetic field such as tunneling magnetoresistance devices [1] or grain boundary (GB) junctions [2–7], are more viable candidates for applications. The tunneling magnetoresistance devices, however, have a disadvantage of involving complex fabrication processes as compared to GB junctions.

In polycrystalline samples, which have GBs in nature, Hwang et al. [8] and Gupta et al. [9] have demonstrated prominent low field MR (LFMR). Their experimental results of increasing LFMR with decreasing grain size imply that the GB

*Corresponding author. Tel.: +88635731943; fax: +88635725230.
E-mail address: sfchen.ep86g@nctu.edu.tw (S.F. Chen).

0921-4526/03/$ - see front matter
doi:10.1016/S0921-4526(03)00261-8

dominates the MR effect [8–10]. Moreover, the observed almost ohmic current voltage characteristics (IVC) evidently suggest that the LFMR might be caused by a combination of spin-scattering and tunneling processes at GBs [11]. In order to analyze the origins of GB MR, various artificial GB samples have been fabricated. For example, the GBs fabricated on bicrystal substrates [2–4], on step-edge substrates [6,12] or in form of biepitaxial films [5]. All these experimental results have demonstrated prominent LFMR and noticeable high field MR (HFMR) below Curie temperature (T_C) due to GBs. In addition, the results of ubiquitously observed non-ohmic IVCs for GBs and the nature of almost spin polarized charge carriers in ferromagnetic state in manganite materials, thus, seem to favor that the inelastic tunneling at GBs is the origin of the observed LFMR [13].

In this study, the samples of $La_{0.7}Ca_{0.3}MnO_3$ (LCMO) biepitaxial films have been fabricated and the MR of the biepitaxial step junction (BSJ) across the boundary layer between two different orientation epitaxial films is investigated. This BSJ demonstrates comparable MR ratio and analogous LFMR and HFMR behaviors with the forementioned artificial GBs [2–7]. However, the IVC is evidently linear. The results are better interpreted by the mechanism of spin-dependent transport across a metallic and depressed magnetic ordering junction layer. The BSJ with characteristics of large LFMR, ohmic IVC and relatively easy fabrication process might be attractive in future applications.

2. Samples and experimental

In order to grow LCMO (1 1 0) and LCMO (0 0 1) films on the same substrate to produce a BSJ, an appropriate buffer layer is needed. Because various CMR and superconducting thin films with predominantly (1 1 0) orientation have been successful deposited on the TiO_2 buffered substrates in our previous studies [14–16], the TiO_2 has been chosen to be the buffer layer in this study. The biepitaxial LCMO thin film samples were prepared on $SrTiO_3$ (0 0 1) (STO) substrates by pulsed laser deposition with half area of the substrate being buffered by a layer of anatase TiO_2. The vertical structure of the sample is schematically illustrated in Fig. 1(a). The TiN thin

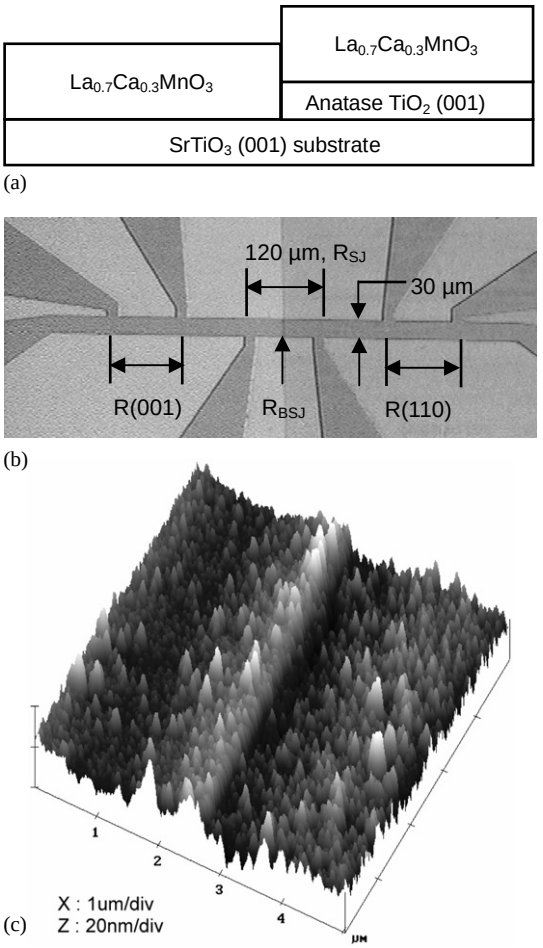

Fig. 1. (a) The vertical structure of biepitaxial films. The TiO_2 buffer layer is in anatase phase and 15 nm in thickness. (b) The microscopic image of the patterned biepitaxial films shown in the same lateral structure order with (a). The BSJ can be clearly seen in the image. The bridge width is 30 μm and the distance between two nearest contact pads is 120 μm. The segment resistance of LCMO (0 0 1) and LCMO (110) film not crossing BSJ are indicated by R(0 0 1) and R(1 1 0), respectively. The measured segment resistance crossing BSJ is indicated by R_{SJ}. The BSJ resistance thus can be obtained by subtracting the thin film resistance not crossing the BSJ to the resistance crossing the BSJ. (c) The atomic force microscopy image in the vicinity of the BSJ region. The sharp BSJ region can be clearly identified. The left and right sides of BSJ are LCMO (1 1 0) and LCMO (0 0 1) films, respectively.

film was first deposited on a STO substrate with the deposition conditions of substrate temperature $T_s = 720°C$ and background pressure of 5×10^{-6} Torr. The half side of TiN film was then removed by wet etching method. The TiO_2 buffer layer having a thickness of about 15 nm was then obtained by oxidizing the sample at 1 atm pure oxygen and 800°C for 30 min. This TiO_2 buffer layer was observed to be anatase phase, instead of rutile phase (see below). The reason could be due to the high oxygen pressure used in oxidizing the TiN film. The LCMO film having a thickness of about 70 nm was deposited on this TiO_2 buffered substrate. The substrate temperature and oxygen pressure (P_{O_2}) during deposition were kept at 720°C and 0.35 Torr, respectively. The sample was then in situ annealed at the same temperature with $P_{O_2} = 600$ Torr for 30 min and then cooled to room temperature at a rate of $-15°C/min$. The LCMO films obtained thus possess two distinct film orientations simultaneously grown on the same STO substrate. A BSJ is formed across the boundary of two regions. It is noted that the LCMO layer was intentionally made thicker than the TiO_2 buffer layer to make BSJ transport the dominant factor of resistance, instead of step-edge transport.

In order to investigate the BSJ resistance, the sample was patterned by wet etching into 30 μm-wide which symmetrically crosses the BSJ with 4 contact pads at each side of the BSJ for four-point probe measurement. The microscopic image of the patterned sample and bridge dimensions are shown in Fig. 1(b). The sample surface and structure were characterized by atomic force microscopy and X-ray diffraction (XRD). Fig. 1(c) shows the atomic force microscopy image in the vicinity of the BSJ. The sharp changes in height clearly identify the BSJ region. Fig. 2 shows the typical $\theta - 2\theta$ XRD patterns for each side of the LCMO film. As in evident from Fig. 2(a) and (b), the LCMO film directly grown on STO (0 0 1) substrate is (0 0 1)-oriented while that grown on TiO_2 buffered region shows predominantly (1 1 0)-oriented structure. These XRD scans indicate both of the biepitaxial film and buffer layer are purely oriented. The full width at half maximum (FWHM) for the LCMO (0 0 1) and LCMO (1 1 0) peaks are about 0.19° and 0.23°. The FWHM for TiO_2 (0 0 4) peak is about 0.54°. All these FWHMs were estimated by Gaussian fit. The reason why the LCMO film grown on an anatase (0 0 l) TiO_2 buffer layer results in (1 1 0) preferred orientation, instead of (0 0 l) orientation, is not clear at present.

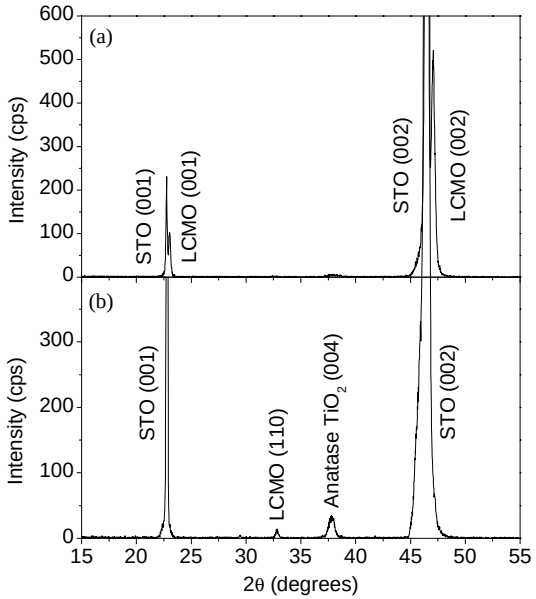

Fig. 2. The X-ray diffraction pattern for (a) the LCMO (0 0 1) and (b) LCMO (1 1 0) films, separately. The purely LCMO (0 0 l) and LCMO (1 1 0) peaks for the respective sides of the biepitaxial films indicate good orientation for each sides.

All transport and magnetic properties were measured using Quantum Design Physical Property Measurement System. The BSJ resistance (R_{BSJ}) is obtained by subtracting the film resistance measured with no crossing of BSJ from that measured across BSJ.

3. Results and discussion

Fig. 3(a) shows the temperature dependent resistance ($R(T)$) obtained from the segments of bridge located within the (0 0 1) and (1 1 0) regions together with the one across the BSJ, indicated in Fig. 1(b) as R(0 0 1), R(1 1 0), and R_{SJ}, respectively. As is seen clearly, the insulator-metal transition

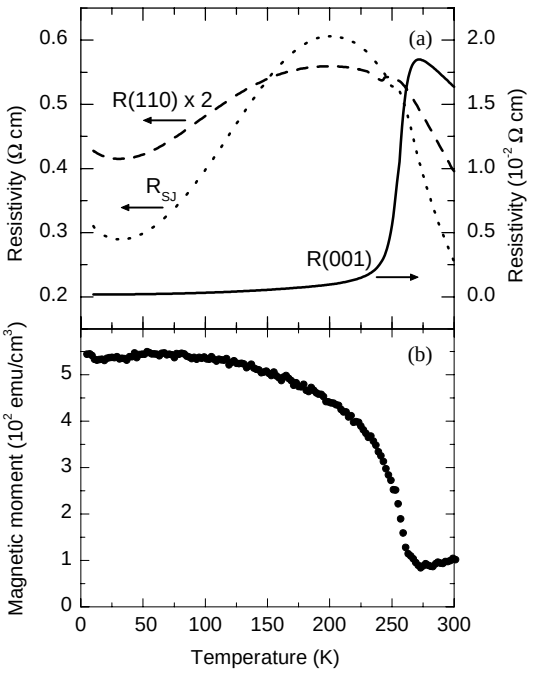

Fig. 3. (a) The resistance plotted as a function of temperature for the LCMO (001) film (denoted as $R(0\,0\,1)$), the LCMO (110) film (denoted as $R(1\,1\,0)$) and the segment crossing BSJ region (denoted as R_{SJ}). (b) Temperature dependence of the magnetic moment of the biepitaxial films. The ferromagnetic transition occurs at 260 K.

temperature (T_{IM}) for $R(0\,0\,1)$ peaks around 265 K, while that for $R(1\,1\,0)$ and R_{SJ} is about 60 K lower with a very broad transition. Despite of the dramatic differences displayed in T_{IM}, it is remarkable to note that the temperature dependent magnetization $M(T)$ measured over the entire bridge displays only one single ferromagnetic transition with a T_C around 260 K, as shown in Fig. 3(b). Although, it is impossible to measure $M(T)$ on the respective segment of the film, there have been evidences from other manganite films deposited on various substrates display a wide range of T_{IM}'s while T_C remained nearly constant [17,18]. It is suggestive that while magnetization may have reflected the intrinsic property, the transport properties appear to be extremely sensitive to the crystalline microstructures. In addition, there are two more peculiar features to be noted in the $R(1\,1\,0)$ and R_{SJ}. Firstly, there is a dip in $R(T)$ around 240 K. This resistance dip has been consistently observed to appear at temperatures near the T_C. However, it is also dependent of measuring history and the strength of the applied field (see below). Mathieu et al. [5] has suggested that it might be due to local magnetic ordering associated with a distributed ferromagnetic transition within grain boundaries. The XRD results shown in Fig. 2 seem to support this extrinsic effect scenario, in that the LCMO (1 1 0) region exhibits relatively poor crystallinity. The second feature is the slightly upturn in $R(T)$ at very low temperatures. This might be, again, due to the relatively poor crystalline ordering-induced weak-localization over the regions covered by segments giving rise to $R(1\,1\,0)$ and R_{SJ}. However, whether both are due to purely extrinsic effects or are something intrinsic to crystalline orientations might need further studies to clarify. Finally, although the similarity of $R(1\,1\,0)$ and R_{SJ} may lead one to ascribe a single prevailing mechanism to the results, we note that R_{SJ} of is more than two-times higher than $R(1\,1\,0)$, which in turn is about another order of magnitude higher than $R(0\,0\,1)$. To simplify the discussion, we will focus on magneto-transport behaviors merely attributed to the BSJ in the following. We thus define $R_{BSJ} \equiv R_{SJ} - 0.5 \times [R(1\,1\,0) + R(0\,0\,1)]$ as the resistance arising from the BSJ.

Fig. 4(a) shows the R_{BSJ} and magnetization as a function of applied field at 75 K in low field regime. Here the scale of low field is usually taken as the field just below the saturation field. In the present case, it is taken as 0.1 T. It is evident that R_{BSJ} peaks at the coercive field (H_c) of the magnetization hysteresis loop with $H_c \approx 150$ Oe and shows a large LFMR with $\Delta R/R_0 \approx 17\%$, where $\Delta R \equiv R_{BSJ}(H) - R_0$ and $R_0 \equiv R_{BSJ}(H_c)$. This closely association between resistance change and magnetic ordering leads the finding that if one normalizes the resistance change ($\Delta R(H)$) to the resistance at H_c and plots it as a function of global magnetization (M_g) normalized to the saturation magnetization (M_s), the data fit quite well with

$$\Delta R(H)/R(H_c) \propto -(M_g/M_s)^2. \quad (1)$$

These features are typical for most grain boundary junctions [10,19] and are attributed to either magnetic inhomogeneity-induced scattering [10]

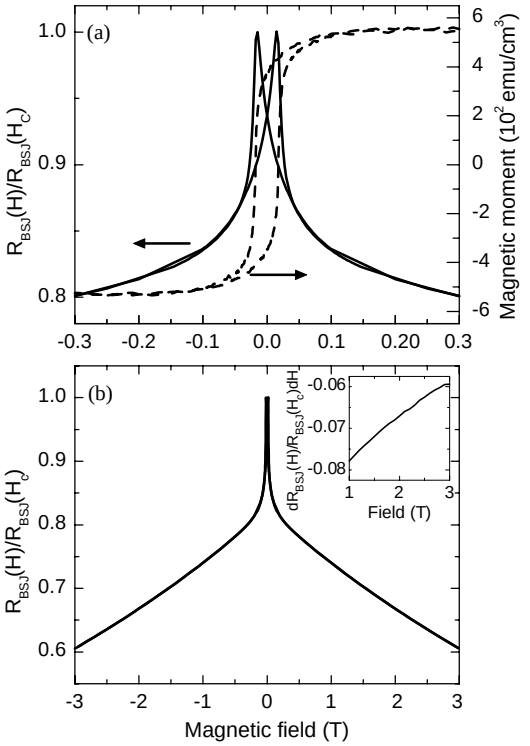

Fig. 4. (a) Magnetic moment of the biepitaxial films plotted as a function of magnetic field at 75 K and the ratio of the field-dependent BSJ resistance $R_{BSJ}(H)$ to the coercive-field value $R_{BSJ}(H_c)$ in the low-field regime. The coercive field is about 150 Oe at 75 K. The coincidence of the R_{BSJ} maximum and the coercive field indicates that the R_{BSJ} is strongly correlated to the magnetic order in films. (b) The $R_{BSJ}(H)/R_{BSJ}(H_c)$ in high-field regime. The inset shows $dR_{BSJ}(H)/R_{BSJ}(H_c)\,dH$ at magnetic field higher than 1 T. The almost linear first derivative indicates the weak H^2 dependence of MR in high field regime.

or intergrain spin-polarized tunneling [8]. In both cases, the alignment of the domains associated with the grains in magnetic field around H_c gives rise to the steep decrease in resistance and predict the same magnetization dependence. Nonetheless, the tunneling model also predicts that there should be no further MR decrease once the magnetization orientation of adjacent grains becoming parallel [6,8,13,20]. However, the ubiquitous HFMR observed on various types of grain boundary junctions often deviates from the prediction significantly [6,13,20]. As shown in Fig. 4(a), typically, the steep decrease of LFMR crosses over to a much slower one, instead of remaining field independent. Although there have been cumulative evidences indicating that linear HFMR [6,13] or linear high field magnetoconductance [21] can be expected and the slope should be proportional to the grain boundary susceptibility χ_{GB} due to inelastic tunneling between ferromagnetic grains via one or two localized states, however, as depicted by the inset of Fig. 4(b), we found that dR/dH in the high field regime is weakly proportional to H^2 plus even higher order terms in H rather than expected linear dependence in H. We have redrawn the Fig. 4(b) in terms of magnetoconductance, however, similar non-linear high field slope has obtained. Alternatively, Evetts et al. [22] proposed that the thermally activated carrier transport within a defective region adjacent to a grain boundary should give rise to a linear HFMR and the magneto-response may be substantially influenced by the grain boundary magnetization. In this scenario, the grain boundary layer is not necessary insulating and the magnetoresistance is in effect the response of a highly disordered mesoscale region with a depressed T_C and magnetization. Although this model is capable of explaining most of the features observed in biepitaxial films, it also predicts a linear HFMR in H. It appears that the ubiquitously observed monotonically decreasing HFMR, though is certainly associated with grain boundary effect, still needs further clarifications.

The characteristics of our BSJ were further identified by measuring the IVCs as functions of temperature and magnetic field. As shown in Fig. 5(a) and its inset, the IVCs across the BSJ segment of the bridge display strictly ohmic behavior over the wide range of temperatures and magnetic fields studied. This is indicative that the current BSJ is indeed metallic in nature, in contrast to most other artificial GBs where various extents of non-ohmic IVCs have been observed and spin-polarized tunneling has been concluded [4,6,12]. Although the slight temperature and magnetic field dependence of the BSJ resistance is consistent with that argued by Evetts et al. [22] Nonetheless, we note that the H^2-dependence of HFMR remains unexplained by various models cited above. Finally, to further delineate the markedly different behaviors exhibited by LFMR

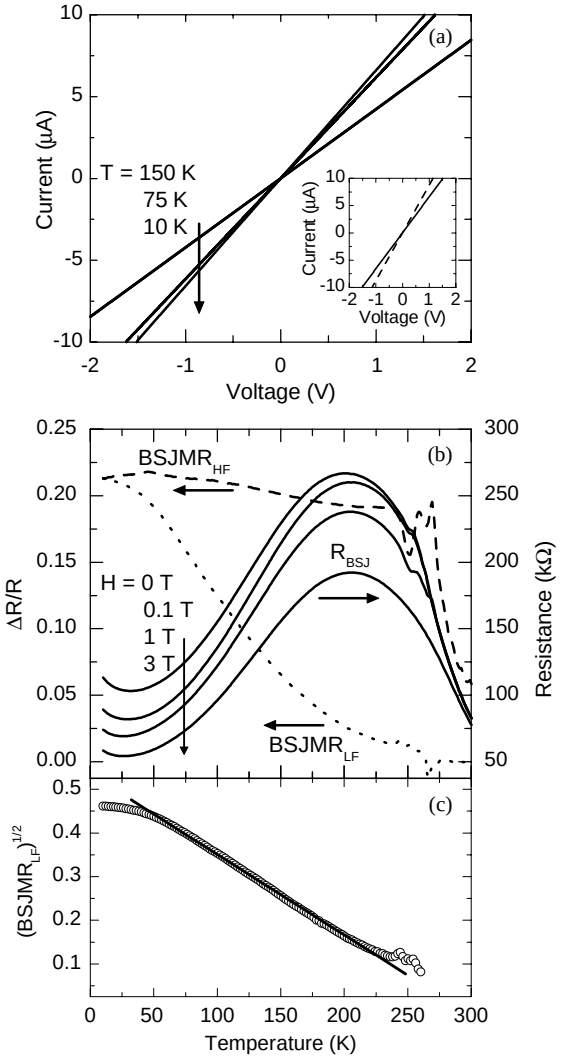

Fig. 5. (a) The IVC's measured for the segment of R_{SJ} at various temperatures and zero magnetic field. The inset shows IVC's measured at 10 K with zero magnetic field (solid line) and $H = 1$ T (dashed line). All IVC's show clear linear current–voltage relationship. (b) Temperature dependence of R_{BSJ} in various magnetic fields (right-hand side axis) and the LFMR ($BSJMR_{LF}$) and HFMR ($BSJMR_{HF}$) of the BSJ (left-hand side axis). The $BSJMR_{LF}$ and $BSJMR_{HF}$ are defined as $[R_{BSJ}(H=0\,T,T)-[R_{BSJ}(H=0.1\,T,T)/[R_{BSJ}(H=0\,T,T)$ and $[R_{BSJ}(H=1\,T,T)-R_{BSJ}(H=3\,T,T)]/R_{BSJ}(H=1\,T,T)$, respectively. (c) The square root of the $BSJMR_{LF}$ plotted as a function of temperature (circles). The $BSJMR_{LF}$ can be fitted well by an equation of $(BSJMR_{LF})^{1/2} = C \times (1 - T/T^*)$ with $C = 0.535$ and $T^* = 290.3$ K (solid line).

and HFMR, we plot the $R(T)$ curves in various fields together with MR ratio ($\Delta R/R$) as a function temperature in low and high field regimes. Here the $BSJMR_{LF}$ and $BSJMR_{HF}$ are defined as $[R_{BSJ}(H=0\,T,T)-R_{BSJ}(H=0.1\,T,T)]/R_{BSJ}(H=0\,T,T)$ and $[R_{BSJ}(H=1\,T,T)-R_{BSJ}(H=3\,T,T)]/R_{BSJ}(H=1\,T,T)$, respectively. Here, we choose 0.1 T to be the field dividing the low-field and high-field regime, because it is the saturation field for magnetization (Fig. 4(a)). As can be seen in Fig. 5(b), the T_{IM} appears to be rather insensitive to the applied magnetic field, however, this is commonly observed in bicrystal GB junctions and epitaxial manganite films [17,20]. Also noticed is that the $R(T)$ behavior remains essentially the same as the field is increased, except for the monotonically decreasing resistance with increasing field. This is indicative of that whatever mechanisms are prevailing for $R_{BSJ}(T)$ the applied fields do not alter them. We note that the $R(T)$ dips near T_C seen in Fig. 3(a) appear to be suppressed at high fields, as well.

The $BSJMR_{LF}$ and $BSJMR_{HF}$ thus reflect the effects of the applied field on $R_{BSJ}(T)$ alone. As described previously, the R_{BSJ} under discussion actually consists of only the resistance resulting from the presence of the step junction. Since the present R_{SJ} is apparently not insulating, our results thus agree with that the junction is indeed consisted of some mesoscale and metallic regions with depressed T_C, as proposed by Evetts et al. [22], instead of insulating regions concluded from the commonly observed results of non-linear IVCs. Furthermore, The $BSJMR_{LF}$ curve shown in Fig. 5(b) between 50 and 230 K can be fitted well by an expression of $(BSJMR_{LF})^{1/2} = C \times (1 - T/T^*)$ with $C = 0.535$ and $T^* = 290.3$ K, as shown in Fig. 5(c). To further discuss this fitting equation, we assume the magnetic moment almost saturates at 0.1 T below T_C, as shown in Fig. 4(a). Hence, the $BSJMR_{LF}$ approximately describes the saturated LFMR. According to Eq. (1), the temperature dependent LFMR should similarly describe the temperature dependence of $(M_g)^2$ if M_s is taken as the saturation magnetization at $T = 0$ K. Thus, if we take the square root of LFMR shown in Fig. 5(c), the magnetization curve shown in Fig. 3(b) would be expected rather than the linear

relationship seen in Fig. 5(c). Alternatively, if we take M_s to be $M_s(T)$ the saturation magnetization at the measuring temperature, then the $[M_g(T)/M_s(T)]^2$ at $H = 0.1$ T would be always approximately unity below T_C. In this scenario, the square root of LFMR describes the temperature dependence of proportional constant in equation (1). Eq. (1) then becomes $(\mathrm{BSJMR_{LF}})^{1/2} = C' \times (1 - T/T^*) \times [M_g(T)/M_s(T)]$. It is suggestive that there may be another mechanism hidden in the proportional constant that determines the temperature dependence of LFMR besides the magnetic ordering. Although the linear relationship has been consistently found on various GB samples [22], the origin is not yet clear and is worthwhile for further investigations.

The $\mathrm{BSJMR_{HF}}$ curve shown in Fig. 5(b) illustrates dramatically increasing at T_C and keeps almost constant below T_C. The result is similar to commonly observed temperature independent HFMR on other types of GBs, however, there is no consistently explanation so far [5,8,13] although HFMR has been attributed to arise from barrier materials in GBs. It is suggestive that the HFMR could be intimately associated with the magnetic order in LCMO films and could be interpreted as follows. The scattering resistance due to the fluctuation of mesoscale junction regions is suppressed by higher field near T_C. Thus, a significant difference in MR appears between 1 and 3 T of applied fields. As the temperature moves further away from T_C, fluctuation reduced and $\mathrm{BSJMR_{HF}}$ reflects purely the difference in M_{BSJ} at different applied fields and is rather insensitive to temperature. We note that the $R(T)$ dips near T_C at several fields may also be explained by magnetization fluctuations and may be turned off by high applied field. In addition, the similar behaviors displayed by the LCMO (1 1 0) region may also arise from similar effects due to its granular features resulting from large lattice mismatches between the buffered-TiO_2 layer and the LCMO film grown on it.

4. Summary

In summary, we have fabricated biepitaxial LCMO films using TiO_2-buffered STO substrates. By intentionally patterning the films into bridges with a step junction connecting regions with different film orientations, we were able to separate the magneto-transport properties from junction region and intra-film regions. A MR value comparable to other structures (about 20%) at low temperatures was obtained. The detailed temperature and field dependence measurements revealed that the magneto-transport of carriers probably is dominated by spin-dependent transport through a metallic-like GB regions rather than spin-polarized tunneling through insulating-like GB regions. In addition, our results are consistent with most of the results previously obtained from similar GBs. We note, however, the detailed mechanisms responsible for the observed LFMR(T) and HFMR(H) remain to be explored.

Acknowledgements

This work was supported by the National Science Council of Taiwan, ROC under Grant Nos: NSC 91-2112-M-009-041 and NSC 91-2212-M-009-046.

References

[1] J.Z. Sun, Phil. Trans. R. Soc. Lond. A 356 (1998) 1693.
[2] S.P. Isaac, N.D. Mathur, J.E. Evetts, M.G. Blamire, Appl. Phys. Lett. 72 (1998) 2038.
[3] K. Steenbeck, T. Eick, K. Kirsch, K. O'Donnell, E. Steinbeiß, Appl. Phys. Lett. 71 (1997) 968.
[4] N. Khare, U.P. Moharil, A.K. Gupta, Appl. Phys. Lett. 81 (2002) 325.
[5] R. Mathieu, P. Svedlindh, R.A. Chakalov, Z.G. Ivanov, Phys. Rev. B 62 (2000) 3333.
[6] M. Ziese, G. Heydon, R. Hohne, P. Esquinazi, J. Dienelt, Appl. Phys. Lett. 74 (1999) 1481.
[7] M. Bibes, B. Martinez, J. Fontcuberta, Appl. Phys. Lett. 75 (1999) 2120.
[8] H.Y. Hwang, S-W. Cheong, N.P. Ong, B. Batlogg, Phys. Rev. Lett. 77 (1996) 2041.
[9] A. Gupta, G.Q. Gong, G. Xiao, P.R. Duncombe, P. Lecoeur, P. Trouilloud, Y.Y. Wang, V.P. Dravid, J.Z. Sun, Phys. Rev. B 54 (1996) R15629.
[10] X.W. Li, A. Gupta, G. Xiao, G.Q. Gong, Appl. Phys. Lett. 71 (1997) 1124.
[11] J.Z. Sun, A. Gupta, Annu. Rev. Mater. Sci. 28 (1998) 45.
[12] M. Ziese, Phys. Rev. B 60 (1999) R738.
[13] M. Ziese, Rep. Prog. Phys. 65 (2002) 143.

[14] S.J. Liu, J.Y. Juang, K.H. Wu, T.M. Uen, Y.S. Gou, J.Y. Lin, Appl. Phys. Lett. 80 (2002) 4202.
[15] S.J. Liu, S.F. Chen, J.Y. Juang, J.-Y. Lin, K.H. Wu, T.M. Uen, Y.S. Gou, Jpn. J. Appl. Phys. 42 (2003) L287.
[16] P.I. Lin, C.W. Liu, C.C. Hsieh, K.H. Wu, J.Y. Juang, T.M. Uen, J.Y. Lin, Y.S. Gou, Jpn. J. Appl. Phys. 40 (2001) L377.
[17] Chun-Che Chen, Alex de Lozanne, Appl. Phys. Lett. 73 (1998) 3950.
[18] A.M. Haghiri-Gosnet, J. Wolfman, B. Mercey, Ch. Simon, P. Lecoeur, M. Korzenski, M. Hervieu, J. Appl. Phys. 88 (2000) 4257.
[19] John Q. Xiao, J. Samuel Jiang, C.L. Chien, Phys. Rev. Lett. 68 (1992) 3749.
[20] R. Gross, L. Alff, B. Buchner, B.H. Freitag, C. Hofener, J. Klein, Y. Lu, W. Mader, J.B. Philipp, M.S.R. Rao, P. Reutler, S. Ritter, S. Thienhaus, S. Uhlenbruck, B. Wiedenhorst, J. Magn. Magn. Mater. 211 (2000) 150.
[21] S. Lee, H.Y. Hwang, Boris I. Shraiman, W.D. Ratcliff II, S-W. Cheong, Phys. Rev. Lett. 82 (1999) 4508.
[22] J.E. Evetts, M.G. Blamire, N.D. Mathur, S.P. Isaac, B.-S. Teo, L.F. Cohen, J.L. Macmanus-Driscoll, Phil. Trans. R. Soc. Lond. A 356 (1998) 1593.